

Spin Vortices and Skyrmions of a Single Electron in Inhomogeneous Magnetic Fields

Amin Naseri,^{1,2} Shenglin Peng,¹ Wenchen Luo,^{1,*} and Jesko Sirker^{2,†}

¹*School of Physics and Electronics, Central South University, Changsha, P. R. China 410083*

²*Department of Physics and Astronomy, University of Manitoba, Winnipeg, Canada R3T 2N2*

(Dated: November 21, 2019)

We study the spin textures of a confined two-dimensional electron in inhomogeneous magnetic fields. These fields can either be external or effective fields due to a background magnetic texture in the plane in which the electron resides. By analytical considerations, WKB-type approximations, and by performing numerical diagonalizations we show that the in-plane spin field components of a single electron can form vortices while the total spin field can become a skyrmion. Most interestingly, we find that topological trivial magnetic fields can induce topological spin field configurations in the eigenstates of the electron due to quantum effects.

I. INTRODUCTION

Pursuing topological phenomena has become one of the main themes in condensed matter physics.¹ In this context, topology refers to the existence of an integer quantity (the topological charge) which is related to the global properties of the system and insensitive to small local perturbations.² In the approach introduced by Michael Berry,³ adiabatically varying the parameters of a model generates an effective magnetic field in its parameter space.⁴ The field is induced by topological charges in close analogy with Dirac monopoles. The Berry phase, which is the observable effect of a topological charge, can be understood as the flux of the emergent field through a surface in parameter space. We demonstrate below that from the Schrödinger equation describing a two-dimensional (2D) electron without a good spin quantum number, current densities can be derived which can be directly related to the topological charge of the spin texture.

The spin of a single electron confined in a quantum dot^{5,6} realizes a quantum bit (qubit) which can encode information^{7,8} and can be used as a building block for a quantum computer.^{9–11} Apart from potential applications, recent experimental progress in controlling a single electron and its confining potential^{12–15} also raises fundamental questions about the spin texture of single electrons in internal effective and applied external magnetic fields. Our study is motivated by the following specific questions: How do the spin fields of a single electron arrange themselves in the presence of a magnetic field with a trivial or non-trivial topological pattern? In a recent work, Ref.16, it has been reported that the in-plane spin texture of the ground state of a 2D electron in a spin-orbit coupled quantum dot can develop a vortex with a topological charge $|q| = 1$. Furthermore, the interplay of spin and the orbital angular momenta of electron vortex beams^{17,18} propagating in a 3D space subject to electric and magnetic fields has been studied theoretically and experimentally.^{19,20} In a setting more relevant to our study, electromagnetic fields with topological patterns have been used to directly manipulate the spin of electron beams.²¹

In this work, the spin texture of an electron strongly confined to a 2D surface is explored in the presence of an inhomogeneous magnetic field $\mathbf{B} = (B_1, B_2, B_3)$.²² The magnetic field \mathbf{B} can represent an external field or the effects of the local magnetic moments of the material which hosts the electron.²³ In the main text, the focus is on the spin textures of eigenfunctions of the 2D system in the presence of spatially dependent inhomogeneous fields. We analyze these textures both analytically and numerically. For magnetic fields which themselves carry a topological charge, the semiclassical Landau-Lifshitz-Gilbert (LLG) equations turn out to be sufficient for this purpose. The spin texture then simply follows the magnetic field—in a similar way small magnetic needles follow the magnetic field lines—and thus also acquires a non-zero topological charge. If the Hamiltonian has a certain rotational symmetry then it is even possible to establish an exact relation between the in-plane spin texture and the topological magnetic field. This relation is in agreement with the LLG equations. More surprisingly, we find that also topologically trivial magnetic fields can induce topological spin textures. In the latter case, it is paramount to consider the interplay between the Zeeman energy and the kinetic energy of the electron. We show that the topological spin patterns which can develop in this case are understood using a Wentzel-Kramers-Brillouin (WKB) approximation.

We consider two classes of topologically trivial magnetic fields: On the one hand, continuous fields which can be thought of as being projections of fields with a topological pattern onto a plane. On the other hand, discontinuous effective fields which might arise due to magnetic domain walls within the plane the electron is confined to. We find that if \mathbf{B} is a trivial field but induces a non-trivial spin texture, then different eigenstates can have different topological numbers. This is in contrast to the case when \mathbf{B} itself has a definite topological pattern in which case all eigenstates have the same topological number as the field. We want to stress that not all of the magnetic fields considered here can be realized as external fields. They rather represent effective magnetic fields originating from the magnetic texture of the background plane which is Hund-coupled²⁴ with the spin of the elec-

tron. In addition, we will also analytically address the possible spin textures due to a uniform magnetic field and internal spin-orbit couplings (see Appendix D). Although our analysis is primarily concerned with the spin texture of a single electron, it is applicable to any spin-1/2 particle.

The manuscript is organized as follows. In Sec. II, we introduce a generic 2D Hamiltonian of an electron in an inhomogeneous magnetic field. Continuity equations for the spin densities and current densities for a generic eigenfunction are presented. This representation also helps to establish identities which connect the topological charges to the charge density, the spin densities, and their current densities. In Sec. III, we discuss the spin textures generated by magnetic fields with a topological charge. The possible spin textures in topologically trivial magnetic fields are presented in Sec. IV. The two different cases, continuous and discontinuous fields, are analyzed in separate subsections. In Sec. V, magnetic fields with different winding numbers in different domains are discussed. A brief summary of our main results and an outlook is given in Sec. VI.

II. PRELIMINARIES

The Hamiltonian H of a non-relativistic electron in a magnetic field is given by

$$H = H_0 + \frac{\Delta}{2} \mathbf{B} \cdot \boldsymbol{\sigma}, \quad (1)$$

where Δ is a Zeeman coupling factor, $\boldsymbol{\sigma} = (\sigma_1, \sigma_2, \sigma_3)$ is the vector of Pauli matrices, and

$$H_0 = \frac{\boldsymbol{\Pi}^2}{2m_e} + V_0. \quad (2)$$

H_0 commutes with all Pauli matrices, $[H_0, \sigma_j] = 0$ for $j = 1, 2, 3$, $\boldsymbol{\Pi} = \mathbf{p} - e\mathbf{A}$ is the mechanical momentum, \mathbf{A} is a vector potential and we use the Coulomb gauge $\nabla \cdot \mathbf{A} = 0$. V_0 is a confining potential. The mass and charge of the electron are m_e and $e < 0$, respectively. In numerical calculations, we use the parameters appropriate for an InAs quantum dot: $m_e = 0.042m_0$ where m_0 is the mass of a free electron, and a Landé factor $g_e = -14$. The two independent energy scales of the theory are the cyclotron energy $\hbar\omega_c = \hbar|e|B_0/m$ and the Zeeman energy ΔB_0 , where B_0 is the unit of magnetic field in our study. Here we will investigate the spin textures of an electron in the quantum regime, in which the eigenfunctions of H govern the physics of the electron.

If $\Psi(\mathbf{r})$ is an eigenfunction of H , then the charge and spin fields are defined by

$$\varrho_\nu \equiv \Psi^\dagger(\mathbf{r})\sigma_\nu\Psi(\mathbf{r}), \quad (3)$$

for $\nu = 0, 1, 2, 3$ where σ_0 is the 2×2 identity matrix, and the position vector—in the plane the electron resides in—is given by $\mathbf{r} = (\rho, \theta)$. Occasionally, we refer

to the fact that the 2D system is embedded in 3D space, i.e., the electron is living at $z = 0$ in a cylindrical coordinate system $\mathbf{r} = (\rho, \theta, z)$. Investigating the non-trivial topology of the in-plane spin field

$$\boldsymbol{\varrho}_\perp(\mathbf{r}) = (\varrho_1, \varrho_2), \quad (4)$$

and the full three-dimensional spin field

$$\boldsymbol{\varrho}(\mathbf{r}) = (\varrho_1, \varrho_2, \varrho_3), \quad (5)$$

is the purpose of this work. We note that $\boldsymbol{\varrho}(\mathbf{r})$ and $\boldsymbol{\varrho}_\perp(\mathbf{r})$ are observables and a unitary transformation of H leaves their topological features invariant.²⁵

We review two simple cases which do not result in a topological pattern in the spin texture. First, if the Hamiltonian is translationally invariant $[H, \mathbf{p}] = 0$, where $\mathbf{p} = -i\hbar\nabla$ is the canonical momentum, then Ψ can be chosen to be a simultaneous eigenfunction of H and \mathbf{p} which leads to $\mathbf{p}\varrho_j = 0$ since $(\mathbf{p}\Psi)^\dagger = -\mathbf{p}\Psi^\dagger$ (i.e. Ψ and Ψ^\dagger have opposite momenta). Second, if there is a good spin quantum number, then by a unitary transformation σ_3 can be chosen to commute with the Hamiltonian $[H, \sigma_3] = 0$, therefore, $\varrho_{1,2} = 0$ and $\varrho_3 = \pm\varrho_0$. We conclude that if the spin texture is non-trivial, then the translational symmetry must be broken and $[H, \boldsymbol{\sigma} \cdot \hat{n}] \neq 0$ must be satisfied for any fixed 3D unit vector \hat{n} .

In the following, the translational symmetry is broken by the inhomogeneous magnetic field and by the confining scalar potential V_0 . The symmetries and the analytical form of the confining potential do not play a role in our results. We assume that the electron is strongly confined to the 2D plane by a potential $m\omega_z^2 z^2/2$ which allows to neglect the degree of freedom perpendicular to the plane. Within the plane, we assume that the electron has confinement lengths $L_{x,y}$.

An eigenfunction of H , which is a spinor, can be formally written as

$$\Psi(\mathbf{r}) = \begin{pmatrix} e^{iS_1}\psi_1 \\ e^{iS_2}\psi_2 \end{pmatrix}, \quad (6)$$

where $S_{1,2}$ and $\psi_{1,2}$ are real functions. The charge and spin densities become

$$\begin{aligned} \varrho_0 &= \psi_1^2 + \psi_2^2, & \varrho_1 &= 2\psi_1\psi_2 \cos(S_2 - S_1), \\ \varrho_2 &= 2\psi_1\psi_2 \sin(S_2 - S_1), & \varrho_3 &= \psi_1^2 - \psi_2^2, \end{aligned} \quad (7)$$

where $\varrho_0 = |\Psi(\mathbf{r})|^2$. For the 3D vector field, it follows immediately that

$$\sum_{j=1}^3 \varrho_j^2 = \varrho_0^2, \quad (8)$$

which implies that the spin is conserved globally

$$\int d^2r |\boldsymbol{\varrho}(\mathbf{r})| = \int d^2r \varrho_0 = 1. \quad (9)$$

Using the representation (6), we find that the phase difference between the two spin components is related to the in-plane spin fields

$$\nabla(S_2 - S_1) = \frac{\varrho_1 \nabla \varrho_2 - \varrho_2 \nabla \varrho_1}{\varrho_1^2 + \varrho_2^2}. \quad (10)$$

The *winding number of the in-plane spin field* is now obtained by requiring that the eigenfunction is single-valued,

$$q = \frac{1}{2\pi} \oint \nabla(S_2 - S_1) \cdot d\mathbf{l}, \quad q \in \mathbb{Z}, \quad (11)$$

where $d\mathbf{l}$ is an element of a closed loop in the $x-y$ plane. If $q = 0$, then the spin field is trivial. If $q \neq 0$, then $\boldsymbol{\varrho}_\perp(\mathbf{r})$ describes a vortex with the topological charge q . If the radius of the loop ρ is taken such that $\rho \gg L_{x,y}$ and the loop encloses all singularities, then we call q the net winding number of the spin configuration. We can understand the relation between the winding number and the Berry connection of the wave function in the special case where the kinetic energy can be ignored and $B_3 = 0$. In this case $\varrho_3 = 0$ and the winding number can be written immediately in terms of a Berry connection

$$A_B = i \langle \Psi_B | \nabla \Psi_B \rangle = \nabla(S_1 - S_2), \quad (12)$$

where we have fixed the gauge by setting

$$|\Psi_B\rangle = \frac{1}{\sqrt{2}} \begin{pmatrix} 1 \\ e^{i(S_2 - S_1)} \end{pmatrix}. \quad (13)$$

On the other hand, we can also consider the topological character of the full three-dimensional spin field $\boldsymbol{\varrho}(\mathbf{r})$. To do so, we define the topological current density

$$\mathbf{J}_t = \bar{\boldsymbol{\varrho}}(\mathbf{r}) \cdot (\partial_x \bar{\boldsymbol{\varrho}}(\mathbf{r}) \times \partial_y \bar{\boldsymbol{\varrho}}(\mathbf{r})), \quad (14)$$

where $\bar{\boldsymbol{\varrho}}(\mathbf{r}) = \boldsymbol{\varrho}(\mathbf{r})/\varrho_0$. The *Skyrmion (Pontryagin) number* of the spin field can then be expressed as

$$Q = \frac{1}{4\pi} \int d^2r J_t. \quad (15)$$

In this article we will investigate both the in-plane winding number q defined in Eq. (11) as well as the Skyrmion number Q which are different in general.

If we know the eigenfunctions Ψ of the Hamiltonian, for example from a numerical calculation, then the spin fields and their topological numbers can be easily calculated. Here we will show that it is possible to understand the topology of the spin textures analytically without having to fully diagonalize the Hamiltonian. In order to do so, we will start from continuity equations for the spin fields^{26,27} which are decompositions of the charge continuity equation in the basis of Pauli matrices. Multiplying the time-dependent Schrödinger equation from the left by $\Psi^\dagger \sigma_\nu$ and taking its imaginary part, we find that the spin current densities

$$\mathbf{J}_\nu = \frac{1}{2m_e} [\Psi^\dagger \sigma_\nu \mathbf{p} \Psi - (\mathbf{p} \Psi^\dagger) \sigma_\nu \Psi] - \frac{e}{m_e} \mathbf{A} \varrho_\nu, \quad (16)$$

obey the continuity equations

$$\nabla \cdot \mathbf{J}_\nu + \partial_t \varrho_\nu = \frac{\Delta}{\hbar} [\mathbf{B} \times \boldsymbol{\varrho}(\mathbf{r})] \cdot \hat{x}_\nu, \quad (17)$$

where \hat{x}_j are unit vectors in a 3D Cartesian coordinate system, and we define $\hat{x}_0 = 0$. For a stationary system, the time derivative of the densities is zero in all the equations, $\partial_t \varrho_\nu = 0$. If there is a good spin quantum number e.g. $[H, \sigma_3] = 0$, all the terms in the continuity equations for $\varrho_{1,2}$ vanish while the continuity equation for the third component of the spin density reduces to the charge density continuity equation $\nabla \cdot \mathbf{J}_0 + \partial_t \varrho_0 = 0$. If the spin is not a good quantum number, then the components of the spin torque play the role of a source/sink in the continuity equations of the spin fields. Since the spin is conserved globally according to Eq. (9), the net contribution of the spin-torque components must vanish. This can be verified as follows

$$\begin{aligned} i\Delta \int d^2r \mathbf{B} \times \boldsymbol{\varrho}(\mathbf{r}) &= \langle \Psi | [\boldsymbol{\sigma}, H] | \Psi \rangle \\ &= \langle \Psi | (\boldsymbol{\sigma} H - H \boldsymbol{\sigma}) | \Psi \rangle = \langle \Psi | \boldsymbol{\sigma} | \Psi \rangle (E - E) = 0, \end{aligned} \quad (18)$$

where E is an eigenenergy of the Hamiltonian, $H|\Psi\rangle = E|\Psi\rangle$. This relation implies $\int d^2r \nabla \cdot \mathbf{J}_\nu = 0$, by taking an integral of Eq. (17) in the static case.

The topological numbers q and Q , defined in Eq. (11) and Eq. (15) respectively, can be rewritten in terms of the current densities, see Appendix A 1 for details. The winding number q is related to \mathbf{J}_0 and \mathbf{J}_3 by

$$q = \frac{m_e}{\pi \hbar} \oint \frac{\varrho_3 \mathbf{J}_0 - \varrho_0 \mathbf{J}_3}{\varrho_0^2 - \varrho_3^2} \cdot d\mathbf{l}, \quad (19)$$

and the topological current density has the form (with a sum over repeated indices implied)

$$\mathbf{J}_t = \frac{\varrho_\nu}{\varrho_0} \eta^{\nu\mu} \frac{b_\mu}{\varrho_0}, \quad (20)$$

where $b_\mu = \frac{m_e}{\hbar} \nabla \times \mathbf{J}_\mu \cdot \hat{z}$, and $\eta^{\nu\mu}$ is the Minkowski metric with a signature $(+, -, -, -)$. It is worth mentioning that the representation of \mathbf{J}_t in Eq. (20) is the Mermin-Ho relation²⁴ for the case $\varrho_0 \neq 1$. These relations suggest that the current densities play the role of vector potentials for the emergent magnetic fields and the spatial integral of the generated flux is the geometrical phase of the theory, see Appendix A 2 for details.

III. MAGNETIC FIELDS WITH A TOPOLOGICAL PATTERN

In this section, we study magnetic fields which themselves do have a non-zero winding or Skyrmion number defined by

$$q_B = \frac{1}{2\pi} \oint \frac{(B_1 \nabla B_2 - B_2 \nabla B_1)}{B_1^2 + B_2^2} \cdot d\mathbf{l}. \quad (21)$$

and

$$Q_B = \frac{1}{4\pi} \int d^2r \bar{\mathbf{B}} \cdot (\partial_x \bar{\mathbf{B}} \times \partial_y \bar{\mathbf{B}}), \quad (22)$$

respectively, where $\bar{\mathbf{B}} = \mathbf{B}/|\mathbf{B}|$. In order to find a relation between the spin densities and the components of the magnetic field, we start from the continuity equations. First, we note that if the Hamiltonian does not have a good spin quantum number but commutes with the following angular-momentum operator

$$J_z^N = \frac{-i}{N} \partial_\theta + \frac{1}{2} \sigma_z, \quad N \in \mathbb{Z} \text{ and } N \neq 0, \quad (23)$$

then the radial and angular degrees of freedom of the eigenfunction Ψ are separable and it can be shown that $\nabla \cdot \mathbf{J}_3 = 0$ (see Appendix B) which gives

$$\varrho_2 B_1 = \varrho_1 B_2. \quad (24)$$

That is, the in-plane spin texture $\boldsymbol{\varrho}_\perp$ exactly follows the in-plane magnetic field \mathbf{B}_\perp , and hosts a vortex with $q = N$. Therefore, it is proper to call the integer number N the vorticity of the rotational symmetry. Among magnetic fields discussed below, the fields in Eqs. (28,29), and (33) used in the Hamiltonian (1) have this symmetry. Hence, the vorticity of the fields in Eqs. (28), (29) and (33) are $N = -n$, $N = n$ for $n \in \mathbb{Z}^+$ and $N = 1$, respectively.

We will now show that the relation (24) remains valid approximately even if J_z^N is not conserved. To do so, we consider the continuity equations at distances far from the origin of the confinement, $\rho \gg L_{x,y}$. In this regime, the bare kinetic energy is much smaller than the potential energies and can be neglected. We further assume an in-plane vector potential $\mathbf{A} = B_0/2(-y, x, 0)$ which gives a uniform magnetic field perpendicular to the plane. The continuity equations (17) then reduce to

$$-\frac{e}{m_e} \mathbf{A} \cdot \nabla \varrho_j = \omega_c \partial_\theta \varrho_j \approx \frac{\Delta}{\hbar} [\mathbf{B} \times \boldsymbol{\varrho}(\mathbf{r})] \cdot \hat{x}_j, \quad (25)$$

where $\omega_c = |e|B_0/(2m_e)$ is the cyclotron frequency. We, furthermore, define the dimensionless $\bar{\omega}_c = \hbar\omega_c/E$ and a dimensionless magnetic field $\tilde{\mathbf{B}} = \Delta\mathbf{B}/E$ where E is the eigenenergy of the eigenstate Ψ we measure the spin fields in. We then treat $\bar{\omega}_c$ as the smallest parameter in the theory and expand the spin fields in a power series in $\bar{\omega}_c$ in the spirit of the WKB approximation

$$\varrho_j = \sum_{n=0}^{\infty} \bar{\omega}_c^n \varrho_j^{(n)}. \quad (26)$$

By setting equal the terms of the same power in $\bar{\omega}_c$ in Eq. (25), the leading-order spin fields are related to the magnetic field by

$$\frac{\varrho_i^0}{\varrho_j^0} = \frac{B_i}{B_j}, \quad (27)$$

given that neither of the components of the magnetic field is identically zero, $B_j \neq 0$. In other words, the spin fields to leading order are aligned with the magnetic field in agreement with what is expected classically and the exact relation in Eq. (24) in the rotationally symmetric case. Given that q_B is unique for all the contours enclosing the origin (and not just those at $\rho \gg L_{x,y}$), the winding number of the induced spin texture is given by $q = q_B$. It is worth noting that all the eigenstates of H have the same net winding number because the above argument is applicable to any generic eigenstate of H . However, Eq. (27) is unable to predict the Skyrminion charge of the spin texture even for a magnetic field \mathbf{B} with $Q_B \neq 0$. Eq. (27) is only valid at $\rho \gg L_{x,y}$ while computing the Skyrminion charge requires to know the polarisation of ϱ_3 at every point of the plane.

We exemplify the validity of Eq. (27) for the following magnetic fields which have a non-trivial topological pattern and induce vortices with $q \in \mathbb{Z}$. These magnetic fields can, on the one hand, arise due to magnetic textures in the plane which are Hund-coupled with the spin of the electron. If, on the other hand, \mathbf{B} is an external magnetic field, then it must be divergence-free, $\nabla \cdot \mathbf{B} = 0$, as we are not interested in analyzing the spin textures of magnetic monopoles. Besides, \mathbf{B} must be curl-free, $\nabla \times \mathbf{B} = 0$, according to the Maxwell equations since the model is taken to be time-independent. The magnetic field

$$\mathbf{B}_n^- = B_0 \left(\frac{\rho}{l}\right)^n (\cos(n\theta), -\sin(n\theta), 0), \quad (28)$$

fulfills the latter conditions and generates a vortex with a charge $q = -n$. Here n is a positive integer $n \in \mathbb{Z}^+$, and $l = \sqrt{\hbar/(m_e\omega)}$ is the confinement length of the potential $V_0 = (1/2)m_e\omega^2\rho^2$. The magnetic field

$$\mathbf{B}_n^+ = B_0 \left(\frac{\rho}{l}\right)^n (\cos(n\theta), \sin(n\theta), zf(x, y)), \quad (29)$$

on the other hand, has an in-plane vortex with a charge $q = n$ and $n \in \mathbb{Z}^+$. $f(x, y)$ is chosen such that the field is divergence-free, where x, y, z are Cartesian coordinates in a 3D space. \mathbf{B}_n^+ , however, can have a non-zero curl, $\nabla \times \mathbf{B}_n^+ \neq 0$, which generates a time-dependent electric field. To remedy this problem, we consider the Hamiltonian in the limit $\hbar\omega_c/E \rightarrow 0$ while $(\Delta B_0)/E$ is kept finite. In this limit, the induced time-dependent electric field and the vector potential vanish and leave a stationary system. The ground-state spin textures of an electron exposed to \mathbf{B}_n^\pm are shown in Fig. 1 and are obtained numerically for $n = \pm 1, \pm 2$.

It is curious to note that the 2D magnetic field \mathbf{B}_n^- can be curl and divergence free but \mathbf{B}_n^+ requires the third field component to satisfy the constraints posed by the Maxwell equations. This difference can be understood as follows: \mathbf{B}_n^- and the in-plane part of \mathbf{B}_n^+ can be written in terms of complex variables $\varepsilon = x + iy$ and $\bar{\varepsilon} = x - iy$ as

$$\mathbf{B}_n^- = \frac{B_0}{l^n} \varepsilon^n, \quad \mathbf{B}_{n\perp}^+ = \frac{B_0}{l^n} \bar{\varepsilon}^n, \quad (30)$$

which shows that in this complex notation both fields are holomorphic²⁵

$$\frac{d}{d\varepsilon}\mathbf{B}_n^- = \frac{d}{d\varepsilon}\mathbf{B}_{n\perp}^+ = 0. \quad (31)$$

On the other hand, if they are required to be simultaneously curl and divergence free, they have to also satisfy

$$\frac{d}{d\varepsilon}\mathbf{B}_n^- = \frac{d}{d\varepsilon}\mathbf{B}_{n\perp}^+ = 0. \quad (32)$$

This condition is trivially satisfied for \mathbf{B}_n^- but it forces the in-plane part of \mathbf{B}_n^+ to be identically zero. Hence, the field \mathbf{B}_n^+ cannot just consist of an x and y component; a non-zero z component is needed.

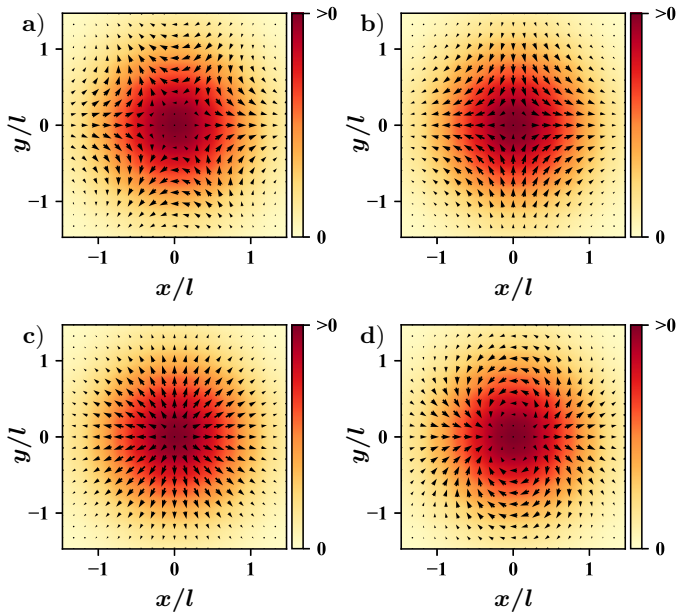


FIG. 1: Ground state in-plane spin textures σ_\perp (arrows) presented on top of a density plot of ϱ_3 . The results are obtained for the non-trivial topological fields \mathbf{B}_n^\pm and a symmetric harmonic confinement $\hbar\omega = 5.0$ meV, and $B_0 = 3.0$ T for **a)** \mathbf{B}_2^- with winding number $q = -2$, **b)** \mathbf{B}_1^- with $q = -1$, **c)** \mathbf{B}_1^+ with $q = 1$, and **d)** \mathbf{B}_2^+ with $q = 2$.

Next, we present the spin texture induced by a Skyrmion magnetic field. The magnetic field of a Skyrmion with $Q_B = -1$ has the form

$$\mathbf{B}^s = B_0 \left(\frac{2\kappa Rx}{\rho^2 + (\kappa R)^2}, \frac{2\kappa Ry}{\rho^2 + (\kappa R)^2}, \frac{\rho^2 - (\kappa R)^2}{\rho^2 + (\kappa R)^2} \right), \quad (33)$$

where κ is a dimensionless parameter and R is a constant with a dimension of length. The spin textures of a few low-energy eigenstates in the presence of the field \mathbf{B}^s are presented in Fig. 2. Although the in-plane winding number is $q = 1$ for all the states, not all of them have the same Skyrmion charges: the third excited state has no Skyrmion while the other states have a Skyrmion with $Q = -1$.

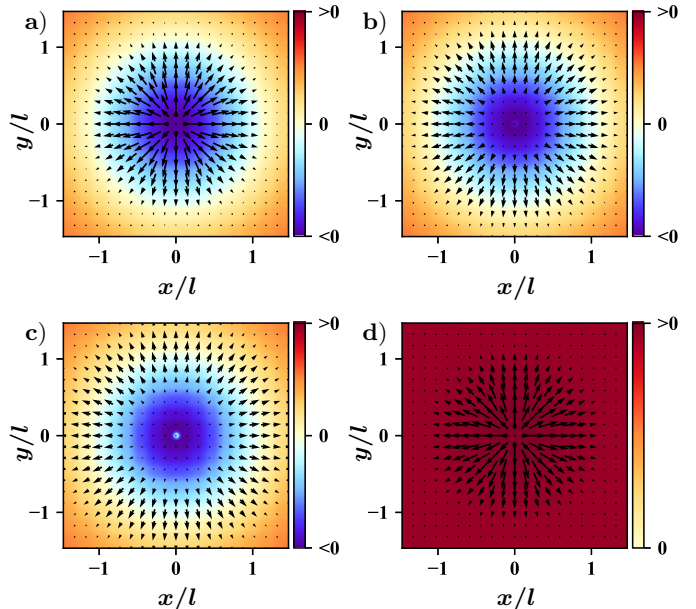


FIG. 2: In-plane spin textures σ_\perp presented on top of the density plot of $\varrho_3 = \varrho_3/\varrho_0$ for the Skyrmion field \mathbf{B}^s with a symmetric harmonic confinement $\hbar\omega = 5.0$ meV, $R = 1.9l$, $B_0 = 7.0$ T and $\kappa = 0.30$. Spin textures in all the eigenstates have $q = 1$, but the ground-state and the first and second excited states have a Skyrmion number $Q = -1$ [see panels **a)**, **b)**, and **c)**] while **d)** the third excited state has no Skyrmion.

IV. MAGNETIC FIELDS WITH A TRIVIAL TOPOLOGICAL PATTERN

In this section, we explore magnetic fields which are topologically trivial in the sense that $q_B = Q_B = 0$ but induce non-trivial spin textures $q \neq 0$ or $Q \neq 0$.

A. Continuous Magnetic Fields

First, we focus on a class of systems experiencing a magnetic field $\mathbf{B}^p = (B_1, 0, B_3)$ with $Q_B = q_B = 0$ which can be thought of as being the projection of a topologically non-trivial field $\mathbf{B} = (B_1, B_2, B_3)$ onto the $x - z$ plane. Our analysis of the continuity equations for this case can qualitatively explain the emergent spin textures. Furthermore, it is in agreement with perturbation theory and exact numerical results, as presented below. We study the continuity equations in the asymptotic limit $\rho \gg L_{x,y}$. The in-plane vector potential is fixed to $\mathbf{A} = (B_0/2)(-y, x, 0)$. The spin continuity equations are then approximated again by Eq. (25). In WKB spirit, we expand the spin fields in the smallest energy scale of the theory $\bar{\omega}_c = \hbar\omega_c/E$, see Eq. (26), and now keep terms up to linear order in $\bar{\omega}_c$. In zeroth order we find $(\tilde{B}_j = \Delta B_j/E)$

$$\varrho_3^{(0)}\tilde{B}_1 = \varrho_1^{(0)}\tilde{B}_3, \text{ and } \varrho_2^{(0)} = 0, \quad (34)$$

which shows that in this semiclassical approximation the spin densities, as expected, follow the magnetic field. Since the magnetic field considered is topologically trivial, the spin fields at this order are topologically trivial as well.

At the first order in $\bar{\omega}_c$ we find

$$\frac{\varrho_1^{(1)}}{\varrho_3^{(1)}} = \frac{\tilde{B}_1}{\tilde{B}_3}, \quad \varrho_2^{(1)} = -\frac{1}{\tilde{B}_3} \partial_\theta \varrho_1^{(0)} = \frac{1}{\tilde{B}_1} \partial_\theta \varrho_3^{(0)}. \quad (35)$$

Thus the fields $\varrho_{1,3}$ still follow the magnetic field. The field ϱ_2 , however, is no longer zero. To solve these equations, we can set $\varrho_{1,3}^{(0)} = \varrho^{(0)} \tilde{B}_{1,3}$ with an unknown function $\varrho^{(0)} \neq 0$. This solves the zeroth order equation (34). Using this lowest order result in the second relation of Eq. (35) and assuming that \tilde{B}_3 is independent of the angle θ we obtain the following differential equation

$$\frac{\tilde{B}_1 \partial_\theta \tilde{B}_1}{\tilde{B}_1^2 + \tilde{B}_3^2} = -\frac{\partial_\theta \varrho^{(0)}}{\varrho^{(0)}} \quad (36)$$

which gives $\varrho^{(0)} = \pm F(\rho) (\tilde{B}_1^2 + \tilde{B}_3^2)^{-1/2}$ where $F(\rho)$ is the radial part of $\varrho^{(0)}$. Using Eq. (35) we can now also determine $\varrho_2^{(1)}$. To lowest non-vanishing order we thus find

$$\begin{aligned} \varrho_3 &= \pm F(\rho) \frac{\tilde{B}_3}{\sqrt{\tilde{B}_1^2 + \tilde{B}_3^2}}, & \varrho_1 &= \pm F(\rho) \frac{\tilde{B}_1}{\sqrt{\tilde{B}_1^2 + \tilde{B}_3^2}}, \\ \varrho_2 &= \mp \bar{\omega}_c F(\rho) \frac{\tilde{B}_3 \partial_\theta \tilde{B}_1}{(\tilde{B}_1^2 + \tilde{B}_3^2)^{3/2}}. \end{aligned} \quad (37)$$

Eq. (37) shows that quantum corrections lead to a non-zero component of the spin-field in y -direction despite the fact that the y -component of the magnetic field \mathbf{B}^p is zero. Therefore a topologically trivial field such as, for example,

$$\mathbf{B}_n^p = B_0 (f(\rho) \cos(n\theta), 0, 1), \quad (38)$$

does generate a vortex in the spin densities (with $|q| = |n|$ in this case). To understand the sign of the winding number, we can treat the x -component of \mathbf{B}_n^p with $f = (b\rho)^{|n|}$ (in which b has a dimension of inverse length) as a perturbation in the Hamiltonian with a symmetric harmonic trap $V_0 = \frac{1}{2} m_e \omega^2 \rho^2$. In the symmetric gauge, the spin fields are then given by

$$\varrho_1 = F_1(\rho) \cos(n\theta), \quad \varrho_2 = \sigma F_2(\rho) \sin(n\theta), \quad (39)$$

for an eigenfunction with spin quantum number $\sigma = \pm 1$ (details for the case $n = 1$ are given in App. C). The winding number of the induced vortex is $q = \sigma n \text{sgn}(F_1 F_2)$ for $F_{1,2} \neq 0$, and can take on $+n$ and $-n$ in different eigenstates. This feature is contrary to the semiclassical cases discussed in the previous section, in which the electron experiences a magnetic field with a non-trivial pattern and the spin textures in *all the eigenfunctions* have an identical topology. If the vector potential is switched off (for instance by considering the regime

$\hbar\omega_c/(\Delta B_0) \rightarrow 0$) in the presence of \mathbf{B}^p , the unperturbed eigenfunctions can be written in terms of Hermite polynomials which are real functions, and the spin texture is thus topological trivial. We note that this is again consistent with the WKB approximation, Eq. (37).

To exemplify the generation of topological spin textures in topologically trivial magnetic fields of the type \mathbf{B}_n^p , we numerically calculate the eigenfunctions for a symmetric harmonic trap V_0 with a length scale $l = \sqrt{\hbar/(m_e \omega)}$. In Fig. 3, the spin textures of the ground state and the first excited state induced by the magnetic field

$$\mathbf{B}_1^p = B_0 \left(\frac{x}{l}, 0, 1 \right), \quad (40)$$

are shown which are vortices with $q = -1$ ($q = 1$) in the ground state (the first excited state), respectively. This field is curl-free and can be made divergence-free by adding a field $B_0 b z \hat{z}$ to \mathbf{B}_1^p , and by noting that the plane in which the electron moves is at $z = 0$. It is interesting to note that the spin texture of the first excited state under \mathbf{B}_1^p is a Skyrmion with $Q = -1$. As a second example, we consider the spin textures induced by

$$\mathbf{B}_2^p = B_0 \left(\frac{xy}{l^2}, 0, 1 \right). \quad (41)$$

As shown in Fig. 4 we now obtain vortices with $q = -2$ ($q = 2$) in the ground state (the first excited state).

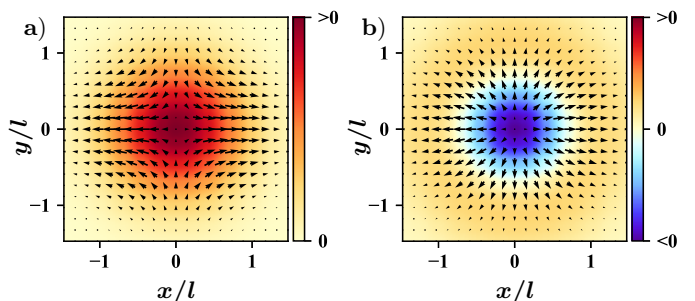


FIG. 3: In-plane spin textures σ_\perp presented on top of the density plot of $\bar{\varrho}_3$ for a model with symmetric harmonic confinement and a magnetic field \mathbf{B}_1^p where $B_0 = 3.0$ T and $\hbar\omega = 5.0$ meV. **a)** The spin texture is a vortex with $q = -1$ in the ground state, and **b)** a Skyrmion with $Q = -1$ and vorticity $q = 1$ in the first excited state.

B. Discontinuous Magnetic Fields

The second type of magnetic fields discussed in this section are discontinuous functions of \mathbf{r} . We are not aiming at presenting a general analysis of all possible kinds of discontinuous fields here but will rather limit ourselves to a couple of helpful examples.

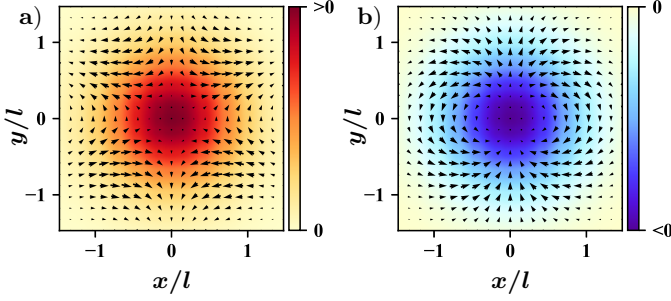


FIG. 4: Same as Fig. 3 but for the field \mathbf{B}_2^p where $B_0 = 2.9$ T and $\hbar\omega = 5.0$ meV. The spin textures are now vortices with **a)** $q = -2$ in the ground state, and **b)** $q = 2$ in the first excited state.

The first example we want to discuss, is a field \mathbf{B}_n^d with components

$$\mathbf{B}_n^d \cdot \hat{x} = \alpha B_0 \left(\Theta(\cos(n\theta)) - \frac{1}{2} \right), \quad (42)$$

$$\mathbf{B}_n^d \cdot \hat{y} = \beta B_0 \left(\Theta(\sin(n\theta)) - \frac{1}{2} \right), \quad (43)$$

where α, β are dimensionless constants and $\Theta(x)$ is the Heaviside step function. Such fields can be thought of as arising from magnetic domains inside the plane to which the electron is confined.^{22,28} The discontinuity of the Heaviside step function $\Theta(x)$ can be smoothed out by using the inverse tangent function $\sim \tan^{-1}(\lambda x)$ instead because the jump at $x = 0$ takes place within a distance which is much smaller than the relevant length scale for the electron, $\lambda L_{x,y} \gg 1$. Using the inverse tangent function instead of the Heaviside step function makes it possible to use Eq. (21) to show that \mathbf{B}_n^d induces an in-plane vortex with winding number $q = n$. In the limit $\lambda L_{x,y} \gg 1$, however, the vector potential \mathbf{A} is required in order to soften the discontinuity. Otherwise, the spin texture is trivial since the spin fields cannot be discontinuous.

It is also possible to turn the spin texture of the electron into a Skyrmion with $|Q| = |n|$ if the z -component of \mathbf{B}_n^d is tailored to

$$\mathbf{B}_n^d \cdot \hat{z} = \gamma B_0 \left(\Theta(\rho/L - \kappa) - \frac{1}{2} \right), \quad (44)$$

where L is a length scale, and κ is a dimensionless constant. Furthermore, it is interesting to note that even after switching off the y -component of \mathbf{B}^d (i.e. $\beta = 0$), the topological spin textures persist as shown in Fig. 5.

As a second example, we present the spin textures of an electron in a hard-wall potential

$$V_{hw} = \begin{cases} 0 & \rho < R, \\ \infty & \rho \geq R, \end{cases} \quad (45)$$

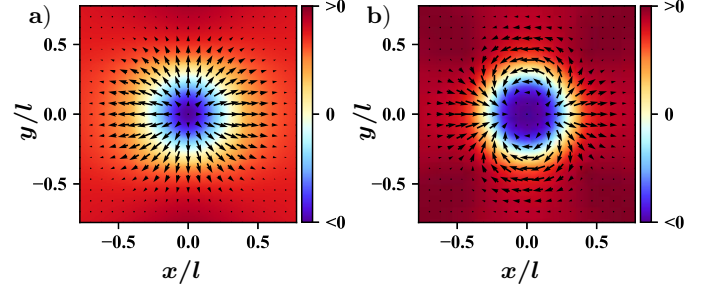


FIG. 5: Ground-state in-plane spin textures σ_{\perp} presented on top of the spin density ϱ_3 for the magnetic field \mathbf{B}_n^d with $L = 36$ nm, $\kappa = 0.32$, $\alpha = 1$, $\beta = 0$, and $\gamma = 2$. Non-zero Skyrmion and winding numbers are found, for example, for **a)** $B_0 = 5.0$ T and $n = 1$, with charges $Q = -1$ and $q = 1$, and **b)** for $B_0 = 7.7$ T, $n = 2$ where $Q = -2$ and $q = 2$.

experiencing the discontinuous in-plane magnetic field

$$\mathbf{B}_{\parallel} = \begin{cases} B_0(-\nu, 0, 0) & y \geq \kappa R, \\ B_0(\mu, 0, 0) & -\kappa R < y < \kappa R, \\ B_0(-\nu, 0, 0) & y \leq -\kappa R, \end{cases} \quad (46)$$

where the domain walls are now parallel to each other rather than radially arranged as in the first example. The parameters chosen to illustrate the spin textures are $\mu = 2$, $\nu = 1$, and $\kappa = 0.15$. We include, furthermore, a uniform magnetic field $\mathbf{B}_0 = B_0 \hat{z}$ perpendicular to the plane which is generated by the vector potential $\mathbf{A} = (B_0/2)(-y, x, 0)$. The spin textures of the ground state and the first excited state for this case are depicted in Fig. 6. A vortex with $q = -2$ is present in the ground state, and a vortex with $q = 2$ in the first excited state. We note that in this setup, the energies confined to each of the domains need to be of the same order of magnitude to favour the formation of vortices.

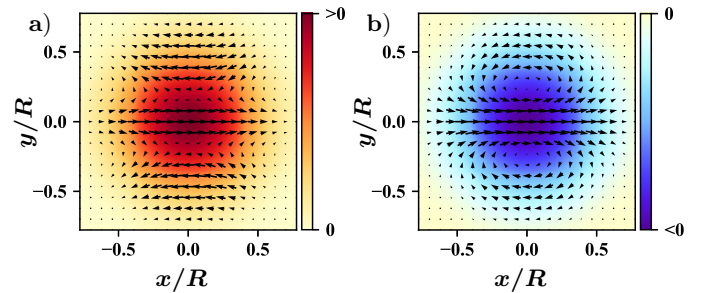


FIG. 6: In-plane spin textures σ_{\perp} presented on top of the spin density ϱ_3 for the magnetic field \mathbf{B}_{\parallel} with $R = 36$ nm as the radius of the potential well, and $B_0 = 2.9$ T. The parameters of the magnetic domain are $\mu = 2$, $\nu = 1$ and $\kappa = 0.15$. The spin texture is a vortex with **a)** $q = -2$ in the ground state, and **b)** with $q = 2$ in the first excited state.

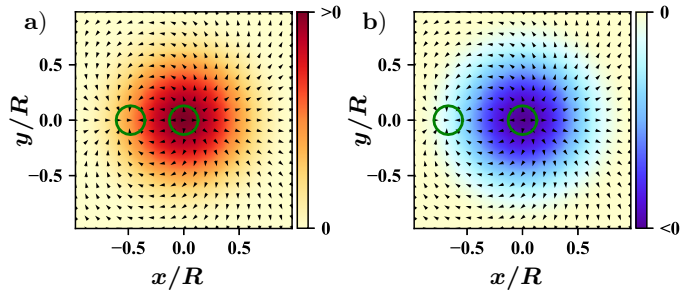


FIG. 7: In-plane spin textures σ_{\perp} presented on top of the spin density ϱ_3 for the magnetic field \mathbf{B}_{12} with $R = 36$ nm as the radius of the potential well, $B_0 = 1.0$ T, $b = 0.25$ R, and $\alpha = \beta = 0.2$. The net winding number is $q = 2$ in **a**) the ground state, as well as **b**) in the first excited state. The vortices, however, now have two singularities. Their positions are indicated by circles.

V. MAGNETIC FIELDS WITH PIECEWISE-DEFINED WINDING NUMBERS

Finally, we will also briefly explore the spin textures in the presence of a magnetic field which in different domains of the plane has a different topological pattern and thus cannot be fully described by a single and unique winding number. This is possible because our theory is not scale free and at different length scales, different fields can be dominant.

We assume the in-plane magnetic field \mathbf{B}_{\perp} in the Hamiltonian is a vector sum of fields and each field has a definite winding number. Equivalently, in terms of ε and $\bar{\varepsilon}$, we write

$$\mathbf{B}_{\perp} = B_0 \sum_{i=1} \left(\frac{\varepsilon}{b_i^+} \right)^{n_i^+} + B_0 \sum_{i=1} \alpha_i^- \left(\frac{\bar{\varepsilon}}{b_i^-} \right)^{n_i^-}, \quad (47)$$

and a finite set of positive integers $\{n_1^{\pm}, n_2^{\pm}, n_3^{\pm}, \dots\}$ defines the magnetic fields and b_i^{\pm} are constants with a dimension of length. The sum of complex variables can be solved locally and be written as a single-term complex variable $\mathbf{B}_{\perp} = B_0 \chi e^{iM\theta}$ where $\chi \equiv \chi(\mathbf{r})$ and M is an integer which is defined locally $M \equiv M(\mathbf{r})$. Eq. (27) can be used to find the winding numbers at different domains. The net winding number is given by the largest n_i^{\pm} . The singularities of the magnetic fields can be found by solving the equation $\mathbf{B}_{\perp} = 0$. However, the singularities of the spin texture can be redistributed since the magnetic fields are renormalized by the terms in the Hamiltonian, for instance the vector potential. As an example, we want to focus on a magnetic field which is a linear combination of two fields, $\mathbf{B}_{12} = \alpha \mathbf{B}_1 + \beta \mathbf{B}_2$ (α and β are dimensionless constants), with different winding numbers q and

$$\mathbf{B}_n = B_0 \left(\frac{\rho}{b} \right)^n (\cos(n\theta), \sin(n\theta), 0). \quad (48)$$

The normalized field $\bar{\mathbf{B}}_{12} = \mathbf{B}_{12}/|\mathbf{B}_{12}|$ gives $q^< = 1$ in

the region $\rho < b\alpha/\beta$ and $q^> = 2$ for $\rho > b\alpha/\beta$, but becomes singular at $\rho = b\alpha/\beta$. An estimate for the position of the singularities of the spin texture can be obtained by solving the equation $\mathbf{B}_{12} = 0$ but this position is, in general, further renormalized depending on the eigenstate of the electron. This is demonstrated in the numerical results shown in Fig. 7. Here the position of the second singularity does indeed change slightly for different eigenstates. We conclude that the simultaneous presence of magnetic fields with different topologies does not necessarily lead to a trivial spin texture, but can rather split the spin texture into different domains. The topological index of each domain is then associated with the one of the dominant field in this domain.

VI. CONCLUSION

Our study shows that topologically non-trivial spin textures of a single confined electron can emerge in the presence of inhomogeneous magnetic fields. This includes in-plane vortices and three-dimensional Skyrmion configurations. The fields can either be applied external fields or effective fields which arise due to a magnetic background in the plane the electron is confined to. Most remarkably, we find that topological spin fields can form even if the magnetic field itself is topologically trivial. This includes the experimentally relevant case of magnetic domain walls.

To understand the spin textures analytically, we started from the continuity equations for the spin fields. At distances large compared to the length scale of the confining potential, the kinetic energy term in the Hamiltonian becomes the smallest energy scale and the continuity equation can be analyzed in the spirit of a WKB approximation. In lowest order—which corresponds to a semiclassical approximation—one finds, as expected, that the spin fields simply follow the magnetic field. A magnetic field which itself has a topologically non-trivial in-plane winding number thus always leads to in-plane spin textures with the same topological index as the field in all of the electronic eigenstates of the system. Interestingly, the same does not apply to the Skyrmion number: Eigenstates of a system in a magnetic field with a non-zero Skyrmion number do not necessarily share this Skyrmion number. Here our WKB approximation turns out to be insufficient because the Skyrmion number is determined by the three-dimensional spin texture across the entire dot. The knowledge of the spin arrangement for distances large compared to the confinement length is not sufficient.

Even more surprisingly, we have demonstrated that quantum corrections—obtained in higher orders of the WKB approximation—can induce topologically non-trivial spin textures for certain topologically trivial magnetic fields. In this case the topological index is, however, not fixed and can vary between different eigenfunctions of the system. The WKB analysis is supported by pertur-

bation theory and exact numerical results. We also examined the case where the magnetic field has a piecewise-defined topological pattern and have argued that the spin texture then also acquires a piece-wise defined topological charge.

Our study is restricted to stationary systems and temperatures $k_B T \ll \hbar\omega$ where thermal fluctuations can be neglected. Topological pattern in the spin density of an electron are, in principle, detectable in experiment. A first step in this direction has been the recent detailed mapping of the charge density of a single electron in a quantum dot.¹⁴ Imprinting topological spin textures in quantum dots using either external magnetic fields or by tailoring domain walls in the plane the electron is confined to, might be an interesting avenue to explore in the search for topological spintronics applications.

VII. ACKNOWLEDGEMENT

W.L. acknowledges support by the NSF-China under Grant No. 11804396. A.N. acknowledges partial financial support by the Canada Research Chairs program through Tapash Chakraborty. A.N. and J.S. acknowledge support by the Natural Sciences and Engineering Research Council (NSERC) through the Discovery Grants program.

Appendix A: Topological densities in terms of current densities

In this appendix, we derive identities which attribute the topological charges to current densities by representing the current densities in terms of the generic eigenfunction (6).

1. Winding number in terms of current densities

First, we define the canonical current as

$$\mathbf{J}_\mu = \frac{\hbar}{2m_e} \tilde{\mathbf{J}}_\mu - \frac{e}{m_e} \mathbf{A} \varrho_\mu, \quad (\text{A1})$$

which have the following forms in term of the the generic eigenfunction given in eq. (6)

$$\tilde{\mathbf{J}}_0 = \varrho_0 \nabla (S_1 + S_2) - \varrho_3 \nabla (S_2 - S_1), \quad (\text{A2})$$

$$\tilde{\mathbf{J}}_1 = \varrho_1 \nabla (S_1 + S_2) - \varrho_2 \nabla \ln \left(\frac{\psi_1}{\psi_2} \right), \quad (\text{A3})$$

$$\tilde{\mathbf{J}}_2 = \varrho_2 \nabla (S_1 + S_2) + \varrho_1 \nabla \ln \left(\frac{\psi_1}{\psi_2} \right), \quad (\text{A4})$$

$$\tilde{\mathbf{J}}_3 = \varrho_3 \nabla (S_1 + S_2) - \varrho_0 \nabla (S_2 - S_1). \quad (\text{A5})$$

The identity $\mathbf{J}_\nu \eta^{\nu\mu} \varrho_\mu = 0$ can be immediately established (summation on repeated indices and the Minkowski metric $\eta^{\nu\mu}$ with the signature $(+, -, -, -)$). Gradients of the

fields have the following forms

$$\nabla \varrho_0 = \varrho_0 \nabla \ln (\psi_1 \psi_2) + \varrho_3 \nabla \ln \left(\frac{\psi_1}{\psi_2} \right), \quad (\text{A6})$$

$$\nabla \varrho_1 = \varrho_1 \nabla \ln (\psi_1 \psi_2) - \varrho_2 \nabla (S_2 - S_1), \quad (\text{A7})$$

$$\nabla \varrho_2 = \varrho_2 \nabla \ln (\psi_1 \psi_2) + \varrho_1 \nabla (S_2 - S_1), \quad (\text{A8})$$

$$\nabla \varrho_3 = \varrho_3 \nabla \ln (\psi_1 \psi_2) + \varrho_0 \nabla \ln \left(\frac{\psi_1}{\psi_2} \right). \quad (\text{A9})$$

These equations can be used to derive the gradient of the phase difference

$$\nabla (S_2 - S_1) = \frac{\varrho_1 \nabla \varrho_2 - \varrho_2 \nabla \varrho_1}{\varrho_1^2 + \varrho_2^2} \quad (\text{A10})$$

$$= \frac{2m_e}{\hbar} \frac{\varrho_3 \mathbf{J}_0 - \varrho_0 \mathbf{J}_3}{\varrho_0^2 - \varrho_3^2}, \quad (\text{A11})$$

where in the second line, the identity $\varrho_\nu \eta^{\nu\mu} \varrho_\mu = 0$ is also used.

2. Skyrmion density in terms of current densities

We use the generic eigenfunction in eq. (6) (though in a different gauge obtained by changing the gauge of the vector potential) in order to write down the topological density in terms of the spin currents. We also use the $SU(2)$ parametrization (ϑ, φ) to write the eigenfunction

$$\tilde{\Psi}(\mathbf{r}) = \begin{pmatrix} \psi_1 \\ e^{iS} \psi_2 \end{pmatrix} = \sqrt{\varrho_0} \begin{pmatrix} \cos(\vartheta/2) \\ e^{i\varphi} \sin(\vartheta/2) \end{pmatrix}, \quad (\text{A12})$$

where $S = S_2 - S_1$ and the vector potential needs to be replaced by $\mathbf{A}' = \mathbf{A} - (\hbar/e) \nabla S_1$. The spin fields become

$$\varrho_1 = \varrho_0 \cos \varphi \sin \vartheta, \quad (\text{A13})$$

$$\varrho_2 = \varrho_0 \sin \varphi \sin \vartheta, \quad (\text{A14})$$

$$\varrho_3 = \varrho_0 \cos \vartheta. \quad (\text{A15})$$

We focus on the canonical part of the current densities $\tilde{\mathbf{J}}'_\mu$ (the prime stands for the new gauge). The Cartesian components of $\tilde{\mathbf{J}}'_\mu$ are (for $k = x, y$)

$$\tilde{J}'_0{}^k = \varrho_0 (1 - \cos \vartheta) \partial_k \varphi, \quad (\text{A16})$$

$$\tilde{J}'_1{}^k = \varrho_0 (\sin \vartheta \cos \varphi \partial_k \varphi + \sin \varphi \partial_k \vartheta), \quad (\text{A17})$$

$$\tilde{J}'_2{}^k = \varrho_0 (\sin \vartheta \sin \varphi \partial_k \varphi - \cos \varphi \partial_k \vartheta), \quad (\text{A18})$$

$$\tilde{J}'_3{}^k = -\tilde{J}'_0{}^k, \quad (\text{A19})$$

The effective magnetic field $b_\mu = \frac{m_e}{\hbar} \nabla \times \mathbf{J}_\mu \cdot \hat{z}$ shall be shown to be responsible for the emergence of a Skyrmion in the spin texture. Separating the canonical parts, the effective field is written as

$$b_\mu = \frac{1}{2} \tilde{b}_\mu - \frac{e}{\hbar} (\partial_x \varrho_\mu A'_y - \partial_y \varrho_\mu A'_x + B_z \varrho_\mu), \quad (\text{A20})$$

where $B_z = \nabla \times \mathbf{A}' \cdot \hat{z}$ and

$$\tilde{b}_\mu = \partial_x \tilde{J}'_y{}^\mu - \partial_y \tilde{J}'_x{}^\mu. \quad (\text{A21})$$

It will be shown that only the canonical parts contribute to the topological density. The explicit form of \tilde{b}_μ for $\mu = 0$ up to 4 are (summation over repeated indices for $p, q = x, y$ is implied)

$$\tilde{b}_0 = (1 - \cos \vartheta) \epsilon_{pq} \partial_p \varrho_0 \partial_q \varphi + \varrho_0 \sin \vartheta \epsilon_{pq} \partial_p \partial_q \varphi, \quad (\text{A22})$$

$$\begin{aligned} \tilde{b}_1 &= \sin \vartheta \cos \varphi \epsilon_{pq} \partial_p \varrho_0 \partial_q \varphi + \sin \varphi \epsilon_{pq} \partial_p \varrho_0 \partial_q \vartheta \\ &\quad - \varrho_0 \cos \varphi (1 - \cos \vartheta) \epsilon_{pq} \partial_p \vartheta \partial_q \varphi, \end{aligned} \quad (\text{A23})$$

$$\begin{aligned} \tilde{b}_2 &= \sin \vartheta \sin \varphi \epsilon_{pq} \partial_p \varrho_0 \partial_q \varphi - \cos \varphi \epsilon_{pq} \partial_p \varrho_0 \partial_q \vartheta \\ &\quad - \varrho_0 \sin \varphi (1 - \cos \vartheta) \epsilon_{pq} \partial_p \vartheta \partial_q \varphi \end{aligned} \quad (\text{A24})$$

$$\tilde{b}_3 = -\tilde{b}_0, \quad (\text{A25})$$

where $\epsilon_{xy} = -\epsilon_{yx} = 1$ and zero otherwise. The following identity

$$\frac{\varrho_\nu}{\varrho_0} \eta^{\nu\mu} \frac{b_\mu}{\varrho_0} = \frac{1}{2} \frac{\varrho_\nu}{\varrho_0} \eta^{\nu\mu} \frac{\tilde{b}_\mu}{\varrho_0}, \quad (\text{A26})$$

is held since $\mathbf{A}' \varrho_\nu \eta^{\nu\mu} \varrho_\mu = 0$ and hence its curl also vanishes. It is straightforward to show the last identity gives the topological density in eq. (20)

$$\mathbf{J}_t = \frac{\varrho_\nu}{\varrho_0} \eta^{\nu\mu} \frac{b_\mu}{\varrho_0} = \sin \vartheta \epsilon_{pq} \partial_p \vartheta \partial_q \varphi, \quad (\text{A27})$$

which is the Mermin-Ho relation.²⁴

Appendix B: Exact relation between spin fields and in-plane magnetic field

We show that if H does not give a good spin quantum number but it has a rotational symmetry $[H, j_z^N] = 0$, where j_z^N is defined by $j_z^N = -i\partial_\theta/N + \sigma_z/2$, for $N \in \mathbb{Z}$ and $N \neq 0$, then $\varrho_1 B_2 = \varrho_2 B_1$ is held exactly. The eigenfunctions and eigenenergy of j_z^N are

$$j_z^N \begin{pmatrix} \mathcal{N}_1 e^{im\theta} \\ \mathcal{N}_2 e^{i(m+N)\theta} \end{pmatrix} = \left(\frac{m}{N} + \frac{1}{2}\right) \begin{pmatrix} \mathcal{N}_1 e^{im\theta} \\ \mathcal{N}_2 e^{i(m+N)\theta} \end{pmatrix}, \quad (\text{B1})$$

for $m \in \mathbb{Z}$ and $\mathcal{N}_{1,2}$ are normalization constant which satisfy $|\mathcal{N}_1|^2 + |\mathcal{N}_2|^2 = 1$.

We choose the generic eigenfunction of H in a gauge given in Eq. (A12), and hence, the vector potential is $\mathbf{A}' = \mathbf{A} - (\hbar/e)\nabla S_1$. In this representation we found $\tilde{\mathbf{J}}'_0 = -\tilde{\mathbf{J}}'_3$, see Eq. (A19), where $\tilde{\mathbf{J}}'_\nu$ is the canonical part of the current density \mathbf{J}_ν . The stationary continuity equations involving $\mathbf{J}_{0,3}$ then read

$$\frac{\hbar}{2m_e} \nabla \cdot \tilde{\mathbf{J}}'_0 - \frac{e}{m_e} \mathbf{A}' \cdot \nabla \varrho_0 = 0, \quad (\text{B2})$$

$$-\frac{\hbar}{2m_e} \nabla \cdot \tilde{\mathbf{J}}'_0 - \frac{e}{m_e} \mathbf{A}' \cdot \nabla \varrho_3 = \frac{\Delta}{\hbar} [\mathbf{B} \times \boldsymbol{\varrho}(\mathbf{r})] \cdot \hat{x}_3. \quad (\text{B3})$$

Summing them up, we find

$$-\frac{e}{m_e} \mathbf{A}' \cdot \nabla (\varrho_0 + \varrho_3) = \frac{\Delta}{\hbar} [\mathbf{B} \times \boldsymbol{\varrho}(\mathbf{r})] \cdot \hat{x}_3. \quad (\text{B4})$$

If H and j_z^N commutes, they can have a simultaneous eigenfunction which implies the problem is separable $\nabla \psi_{1,2} \parallel \hat{\rho}$ and $\nabla S_{1,2} \parallel \hat{\theta}$. Given $[H, j_z^N] = 0$ implies also the vector potential \mathbf{A} is rotationally invariant, we have $\mathbf{A}' \cdot \nabla (\varrho_0 + \varrho_3) = 0$ which shows that the relation $\varrho_2/\varrho_1 = B_2/B_1$ is exact.

Appendix C: A perturbation theory

In this section, we derive the spin texture of a confined 2D electron in the presence of a homogeneous magnetic field and treat the in-plane magnetic field $H' = (\Delta/2)B_0 b \rho \cos(\theta) \sigma_x = (\Delta/2)B_0 b x \sigma_x$ within a perturbation theory. The unperturbed Hamiltonian is

$$H_0 = \frac{(\mathbf{p} - e\mathbf{A})^2}{2m_e} + \frac{1}{2} m_e \omega^2 \rho^2 + \frac{\Delta B_0}{2} \sigma_z. \quad (\text{C1})$$

where $\mathbf{A} = (B_0/2)(-y, x)$, the electron charge $e < 0$, ω is the confinement frequency, Δ is a coupling factor, the electron g factor is g_e , μ_B is the Bohr magneton, B_0 is a constant with a dimension of magnetic field, and b has a dimension of inverse length. Eigenfunctions of H_0 are

$$\Phi_{n_+ n_-}^\sigma = R_{n_-}^{n_+} e^{i(n_- - n_+) \theta} |\sigma\rangle, \quad (\text{C2})$$

where $\sigma = \pm 1$ is the spin eigenvalue, $n_\pm \in \mathbb{Z}^+ \cap \{0\}$ are the principal quantum numbers, and the radial part of the eigenfunction is

$$R_{n_-}^{n_+} = \mathcal{N}_{n_-}^{n_+} e^{-\rho^2/2\ell^2} \left(\frac{\rho}{\ell}\right)^{n_- - n_+} L_{n_+}^{n_- - n_+} \left(\frac{\rho^2}{\ell^2}\right), \quad (\text{C3})$$

where $L_\lambda^\kappa(x)$ is the associated Laguerre polynomial, $\ell = \sqrt{\hbar/(m_e \Omega)}$, $\Omega = \sqrt{\omega^2 + \omega_c^2}$ and $\omega_c = |e|B_0/(2m_e)$. The normalization factor is

$$\mathcal{N}_{n_-}^{n_+} = \frac{(-1)^{n_+}}{\sqrt{\pi} \ell} \sqrt{\frac{n_+!}{n_-!}}. \quad (\text{C4})$$

The corresponding eigenenergies are

$$E_{n_+ n_-}^\sigma = \sum_{k=\pm} \hbar \Omega_k \left(n_k + \frac{1}{2}\right) + \frac{\Delta}{2} \sigma, \quad (\text{C5})$$

where $\Omega_\pm = \Omega \pm \omega_c$. Treating $H' = (\Delta/2)B_0 b x \sigma_x$ in a first order perturbation theory, the eigenfunction $\Phi_{n_+ n_-}^\sigma$ is modified to

$$\tilde{\Phi}_{n_+ n_-}^\sigma = \Phi_{n_+ n_-}^\sigma + \frac{1}{2} \sum_{k_+, k_-} \alpha_{k_+, k_-}^{n_+, n_-} \Phi_{k_+ k_-}^{-\sigma}, \quad (\text{C6})$$

while the non-zero coefficients are

$$\alpha_{n_-}^{n_+ + 1} = \frac{\Delta B_0 b \ell \sqrt{n_+ + 1}}{\Delta B_0 \sigma - \hbar \Omega_+}, \quad (\text{C7})$$

$$\alpha_{n_-}^{n_+ - 1} = \frac{\Delta B_0 b \ell \sqrt{n_+}}{\Delta B_0 \sigma + \hbar \Omega_+}, \quad (\text{C8})$$

$$\alpha_{n_- + 1}^{n_+} = \frac{\Delta B_0 b \ell \sqrt{n_- + 1}}{\Delta B_0 \sigma - \hbar \Omega_-}, \quad (\text{C9})$$

$$\alpha_{n_- - 1}^{n_+} = \frac{\Delta B_0 b \ell \sqrt{n_- + 1}}{\Delta B_0 \sigma + \hbar \Omega_-}. \quad (\text{C10})$$

The induced spin fields via the perturbation are

$$\varrho_1 = F_1^{n_+n_-} \cos(\theta), \quad (\text{C11})$$

$$\varrho_2 = \sigma F_2^{n_+n_-} \sin(\theta), \quad (\text{C12})$$

with the auxiliary functions

$$F_1^{n_+n_-} = R_{n_+}^{n_+} \sum_{k_+, k_-} \alpha_{k_-}^{k_+} R_{k_-}^{k_+},$$

$$F_2^{n_+n_-} = R_{n_+}^{n_+} \sum_{k_+, k_-} (k_- - k_+ - n_- + n_+) \alpha_{k_-}^{k_+} R_{k_-}^{k_+}.$$

If $\Delta B_0 < \hbar\Omega_{\pm}$, then the states with the same n_{\pm} but opposite spin quantum numbers have winding numbers which differ in sign $q = \pm 1$ in the presence of the perturbation.

Appendix D: Spin-orbit couplings

The spin texture of confined electrons in a 2D space subject to Rashba or Dresselhaus spin-orbit coupling (SOC) hosts a spin vortex with $|q| = 1$.^{16,29} We use Eq. (27) to count the winding number of the vortices. The following Hamiltonian describes a 2D electron in the presence of SOC and a homogeneous magnetic field

$$H_{SOC} = H_0 + g_1 ([p_y - eA_y] \sigma_x - [p_x - eA_x] \sigma_y) \quad (\text{D1}) \\ + g_2 ([p_y - eA_y] \sigma_y - [p_x - eA_x] \sigma_x) + \frac{\Delta}{2} B_0 \sigma_z,$$

where H_0 is given in Eq. (2), $\mathbf{A} = (A_x, A_y, 0) = (B_0/2)(-y, x, 0)$ is the vector potential, the strength of Rashba (Dresselhaus) term is determined by g_1 (g_2), and Δ is a coupling constant. Due to the broken translational symmetry, the electron has confinement lengths $L_{x,y}$. Therefore, the density of momentum decays to zero for distances larger than the confinement lengths $\rho \gtrsim L_{x,y}$ and can be neglected in comparison to the other terms in the Hamiltonian. Neglecting the derivative terms in H_{SOC} in the asymptotic regime, we have

$$\tilde{H}_{SOC} = \tilde{H}_0 - eg_1 (A_y \sigma_x - A_x \sigma_y) \quad (\text{D2}) \\ - eg_2 (A_y \sigma_y - A_x \sigma_x) + \frac{\Delta}{2} B_0 \sigma_z,$$

where \tilde{H}_0 also does not include derivative terms. The effective magnetic fields at $\rho \gg L_{x,y}$ associated with the SOC are then

$$\mathbf{B}_R = -eg_1 (A_y, -A_x, 0), \quad (\text{D3}) \\ \mathbf{B}_D = -eg_2 (-A_x, A_y, 0).$$

Putting these effective fields into Eq. (27), the winding number for the Rashba-dominant SOC (i.e. $g_1 > g_2$) is $q_R = +1$, for the case of Dresselhaus-dominant SOC (i.e. $g_1 < g_2$) is $q_D = -1$, and for $g_1 = g_2$ the winding number vanishes. Since the spin densities are observables, the results are independent of the gauge of the vector potential.

* Electronic address: luo.wenchen@csu.edu.cn

† Electronic address: sirker@physics.umanitoba.ca

¹ Davide Castelvecchi, Nature **547**, 272-274 (2017).

² D. J. Thouless, *Topological Quantum Numbers in Nonrelativistic Physics* (World Scientific, River Edge, N.J., 1998).

³ M. V. Berry, Proc. R. Soc. London A **392**, 45 (1984).

⁴ D. Xiao, M.-C. Chang, and Q. Niu, Rev. Mod. Phys. **82**, 1959 (2010).

⁵ Yu.V. Nazarov and Ya.M. Blanter, Quantum Transport: Introduction to Nanoscience (Cambridge University Press, Cambridge, England, 2009).

⁶ S.M. Reimann and M. Manninen, Rev. Mod. Phys. **74**, 1283 (2002).

⁷ D. Loss and D. P. DiVincenzo, Phys. Rev. A **57**, 120 (1998).

⁸ J. J. Pla, K. Y. Tan, J. P. Dehollain, W. H. Lim, J. J. L. Morton, D. N. Jamieson, A. S. Dzurak, and A. Morello, Nature **489**, 541 (2012).

⁹ I. Zutic, J. Fabian, and S. Das Sarma, Rev. Mod. Phys. **76**, 323 (2004).

¹⁰ L. Smejkal, Y. Mokrousov, Binghai Yan, and A. H. MacDonald, Nat. Phys. **14**, 242 (2018).

¹¹ O. Gomonay, T. Jungwirth, and J. Sinova, Phys. Stat. Sol. RRL **11**, 1700022 (2017).

¹² David D. Awschalom, Lee C. Bassett, Andrew S. Dzurak, Evelyn L. Hu, Jason R. Petta, Science **339**, 6124, (2013).

¹³ K. C. Nowack, F. H. L. Koppens, Yu. V. Nazarov, L. M. K. Vandersypen, Science **318**, 5855, (2007).

¹⁴ L. C. Camenzind, L. Yu, P. Stano, Zimmerman, A. C. Gossard, D. Loss, and D. M. Zumbühl, Phys. Rev. Lett. **122**, 207701 (2019).

¹⁵ P. Stano, C.-H. Hsu, L. C. Camenzind, L. Yu, Dominik Zumbühl, and D. Loss, Phys. Rev. B **99**, 085308 (2019).

¹⁶ Wenchen Luo, Amin Naseri, Jesko Sirker, Tapash Chakraborty, Sci. Rep. **9**, 672 (2019).

¹⁷ K. Y. Bliokh, I. P. Ivanov, G. Guzzinati, L. Clark, R. Van Boxem, A. Béché, R. Juchtmans, M. A. Alonso, P. Schattschneider, F. Nori, J. Verbeeck, Phys. Rep. **690** (2017).

¹⁸ S. M. Lloyd, M. Babiker, G. Thirunavukkarasu, and J. Yuan, Rev. Mod. Phys. **89**, 035004 (2017).

¹⁹ K. Y. Bliokh, Y. P. Bliokh, S. Savel'ev, and F. Nori, Phys. Rev. Lett. **99**, 190404 (2007).

²⁰ M. Uchida and A. Tonomura, Nature **464**, 737 (2010).

²¹ E. Karimi, L. Marrucci, V. Grillo, and E. Santamato, Phys. Rev. Lett. **108**, 044801 (2012).

²² A. Nogaret, J. Phys. Condens. Matter **22**, 253201 (2010).

²³ A. C. Hewson, *The Kondo Problem to Heavy Fermions* (Cambridge University Press, Cambridge, U.K., 1993).

²⁴ Jung Hoon Han, *Skyrmions in Condensed Matter*, (Springer International Publishing, 2017).

²⁵ M. Nakahara, *Geometry, Topology and Physics* (IOP, Bris-

- tol, 1990).
- ²⁶ Junren Shi, Ping Zhang, Di Xiao, and Qian Niu, Phys. Rev. Lett. **96**, 076604 (2006).
- ²⁷ Z. An, F. Q. Liu, Y. Lin and C. Liu, Sci. Rep. **2**, 388 (2012).
- ²⁸ F. M. Peeters and A. Matulis, Phys. Rev. B **48**, 15166 (1993).
- ²⁹ Wenchen Luo and Tapash Chakraborty, Phys. Rev. B **100**, 085309 (2019).